Thin Solid Films 517 (2009) 5537–5542

Contents lists available at ScienceDirect

Thin Solid Films

journal homepage: www.elsevier.com/locate/tsf

Characterizations of gallium-doped ZnO films on glass substrate prepared by atmospheric pressure metal-organic chemical vapor deposition

Yen-Chin Huang [a], Zhen-Yu Li [b], Hung-hsin Chen [a], Wu-Yih Uen [a,*], Shan-Ming Lan [a], Sen-Mao Liao [a], Yu-Hsiang Huang [c], Chien-Te Ku [c], Meng-Chu Chen [c], Tsun-Neng Yang [c], Chin-Chen Chiang [c]

[a] Department of Electronic Engineering, College of Electrical Engineering and Computer Science, Chung Yuan Christian University, Chung-Li 32023, Taiwan
[b] Department of Photonics & Institute of Electro-Optical Engineering, National Chiao Tung University, 1001 TA Hsueh Road, Hsinchu 30010, Taiwan
[c] Institute of Nuclear Energy Research, P.O. Box 3-11, Lungtan 32500, Taiwan

ARTICLE INFO

Article history:
Received 23 May 2008
Received in revised form 17 March 2009
Accepted 23 March 2009
Available online 22 April 2009

Keywords:
Chemical vapor deposition (CVD)
Electrical properties and measurements
Gallium
Optical properties
Scanning electron microscopy
Water
X-ray diffraction
Zinc oxide

ABSTRACT

Ga-doped zinc oxide (ZnO:Ga) films were grown on glass substrate by atmospheric pressure metal-organic chemical vapor deposition (AP-MOCVD) using diethylzinc and water as reactant gases and triethyl gallium (TEG) as an n-type dopant gas. The structural, electrical and optical properties of ZnO:Ga films obtained at various flow rates of TEG ranging from 1.5 to 10 sccm were investigated. X-ray diffraction patterns and scanning electron microscopy images indicated that Ga-doping plays an important role in forming microstructures in ZnO films. A smooth surface with a predominant orientation of (101) was obtained for the ZnO:Ga film grown at a flow rate of TEG = 7.5 sccm. Moreover, a lowest resistivity of 3.6×10^{-4} Ω cm and a highest mobility of 30.4 $cm^2\ V^{-1}\ s^{-1}$ were presented by the same sample, as evaluated by Hall measurement. Otherwise, as the flow rate of TEG was increased, the average transmittance of ZnO:Ga films increased from 75% to more than 85% in the wavelength range of 400–800 nm, simultaneously with a blue-shift in the absorption edge. The results obtained suggest that low-resistivity and high-transparency ZnO films can be obtained by AP-MOCVD using Ga-doping sufficiently to make the films grow degenerate and effect the Burstein–Moss shift to raise the band-gap energy from 3.26 to 3.71 eV.

1. Introduction

Zinc oxide (ZnO) is a wide band gap semiconductor with a hexagonal wurtzite structure. It demonstrates high thermal and chemical stability, good electrical conductivity and high optical transparency. In addition, it also exhibits the features of non-toxicity, low cost and high abundance, and therefore can be considered for widespread applications, such as a transparent conductive layer and/or an antireflection coating for amorphous-silicon (a-Si) and Cu(InGa)Se_2-based solar cells [1–3]. Moreover, ultra-violet light emitting devices based on this material are also possible. Undoped ZnO films usually show n-type conductivity but with a high resistivity due to the intrinsic defects of oxygen vacancies and zinc interstitials [4]. Therefore, high conductive films can be obtained only by doping metal elements that substitute zinc sites [5,6]. Compared to undoped ZnO, the doped one has a lower resistivity and better stability of electrical properties. It is well known that group III elements such as Al [7], In [8], Ga [9] and B [10] act as donors in ZnO. Among these metal dopants, Ga seems to be a promising one because the covalent bond length of Ga–O (0.192 nm) is slightly smaller than that of Zn–O (0.197 nm) and only small ZnO lattice deformations are caused even high concentrations of Ga are introduced.

For the deposition of Ga-doped ZnO (ZnO:Ga) films, a number of growth techniques such as, sol–gel techniques [11], spray pyrolysis [12,13], magnetron sputtering [14–17], pulsed laser deposition [18,19], molecular beam epitaxy [20], ion plating [21], atmospheric pressure metal-organic chemical vapor deposition (AP-MOCVD) [22], plasma enhanced metal-organic chemical vapor deposition [23], and low-pressure metal-organic chemical vapor deposition [24,25] were used. In our study, we fabricate ZnO:Ga films on glass substrates using a two-step AP-MOCVD. Little has been known about the growth of ZnO:Ga film by this method. As is known, AP-MOCVD is a simple fabrication process and cost-competitive for device applications of the ZnO:Ga films. It is capable of producing high growth rates over large areas. Doped films can be deposited by introducing the dopant into the gas phase, and the extent of doping can be easily controlled by the concentration of dopant in gas phase. On the other hand, for being used as transparent electrodes in opto-electronic device applications, thin conducting oxides with an optical transmittance of more than 80% of visible radiation and low resistivity values (10^{-3} to 10^{-4} Ω cm) are required [26]. Table 1 summarizes some recent progress concerning the quality of ZnO:Ga films produced by MOCVD. Compared to these results, the ZnO:Ga films analyzed in this work exhibit sufficiently low resistivity (3×10^{-4} Ω cm) and high transparency (>85%),

* Corresponding author. Tel.: +886 3 265 4620; fax: +886 3 265 4699.
E-mail addresses: uenwuyih@ms37.hinet.net (W.-Y. Uen), chin099983@hotmail.com (C.-C. Chiang).

0040-6090/$ – see front matter © 2009 Elsevier B.V. All rights reserved.
doi:10.1016/j.tsf.2009.03.194

Table 1
Summary of the progress in ZnO:Ga films produced by MOCVD.

Ref	Method	Substrate	Carrier concentration (cm^{-3})	Mobility ($cm^2/V\ s$)	Resistivity (Ω cm)	Transmittance (%)
[27]	LP-MOCVD	Glass	4×10^{21}	6.01	2.6×10^{-4}	>85
[28]	AP-MOCVD	Glass	3.47×10^{20}	60	3×10^{-4}	~85
[29]	LP-MOCVD	Sapphire	2.47×10^{19}	–	–	>90
[30]	LP-MOCVD	ZnO	1.65×10^{21}	27.4	2.21×10^{-4}	>90

and can be considered to be used as a transparent electrode for light-emitting devices. In addition, these films present a high band-gap energy of 3.7 eV, which will also be beneficial for them to be used as a window layer for thin-film solar cells and contribute to an improvement in the device performance. It can be said that ZnO:Ga films with analogous quality have been fabricated on the glass substrate by a simpler method, which is cost competitive for the future applications. In the present work, we characterize ZnO:Ga thin films doped to different degrees to find an optimal condition for Ga-doping and examine the influence of Ga impurity on the structural, electrical and optical properties of ZnO film.

2. Experiments

ZnO thin films were deposited on glass substrate by a homemade AP-MOCVD system. The growth chamber is a water-cooled vertical reactor. The substrate susceptor is made of graphite, 2 in. in diameter and coated with a SiC film on top surface by CVD technique. Diethylzinc (DEZn) and water were used as the sources of Zn and O, respectively. Besides, triethyl gallium (TEG) was used as the doping gas for Ga. N_2 was used as the carrier gas for the growth of ZnO:Ga films. The two-step AP-MOCVD process was conducted as follows. Before the growth of top ZnO:Ga film, an undoped ZnO layer of about 10–20 nm was grown at a low temperature of 170 °C and with a gas flow ratio of [H_2O]:[DEZn] (VI/II ratio) = 13.69, which was used as a buffer for the ZnO:Ga top layers. For the growth of ZnO:Ga top layer, the growth temperature and VI/II ratio were kept at 400 °C and 2.74, respectively, and the growth time duration was set for 30 min to achieve a thickness of about 500–600 nm. The thickness of ZnO films were measured from the cross-sectional scanning electron microscopy (SEM) images of them. Specimens for comparison were fabricated only with different flow rates of TEG ranging from 1.5 to 10 sccm for Ga-doping. The doping effect was confirmed using secondary ion mass spectroscopy (SIMS, Cameca 6f).

The crystalline structure of ZnO:Ga films was analyed by powder X-ray diffraction (XRD, Bruker AXS Diffraktometer D8) using Cu K_α line as the X-ray source ($\lambda = 1.54056$ Å) for a 2θ range 20–80°. The surface morphology of ZnO:Ga films was observed using a scanning electron microscope (SEM, JEOL-6700F) at an accelerating voltage of 10 kV. The resistivity, carrier concentration and mobility of films were measured at room temperature by Hall measurements using the van der Pauw method. Optical transmission spectra were recorded at room temperature using an ultraviolet–visible spectrometer (VARIAN Cary-IE).

3. Results and discussion

Fig. 1 shows a typical SIMS depth profile of Ga concentration along the thickness direction of a ZnO:Ga film fabricated with a TEG flow rate of 7.5 sccm. The average Ga concentration for the whole film estimated on the basis of SIMS data is about 5.74×10^{20} atoms/cm^{-3}, which is in good agreement with the carrier concentration of the same sample (5.66×10^{20}) obtained from Hall measurement described in detail in the following. This fact demonstrates an efficient doping of Ga into the ZnO films using AP-MOCVD.

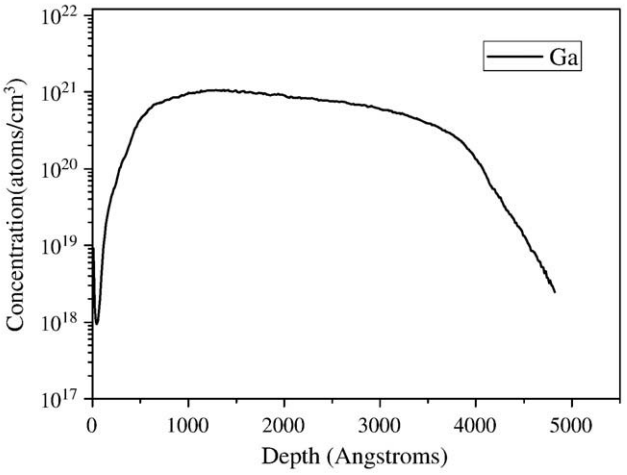

Fig. 1. SIMS depth profile of Ga concentration for ZnO:Ga films fabricated with a TEG flow rate of 7.5 sccm.

Fig. 2(a) and (b) shows the respective surface morphologies of ZnO films grown with and without a ZnO buffer layer, as observed by SEM. As can be seen, the ZnO film grown with a buffer exhibits a relatively homogeneous grain structure compared to that grown without a buffer. This result might manifest that the low-temperature-grown ZnO buffer is required to achieve a continuous overlayer on glass substrate by AP-MOCVD, which is different from the film growth conducted by regular low-pressure MOCVD. The growth of buffer layer also seems to dominate the preferential grain orientation of the top layer, however, more studies should be conducted to realize the related details.

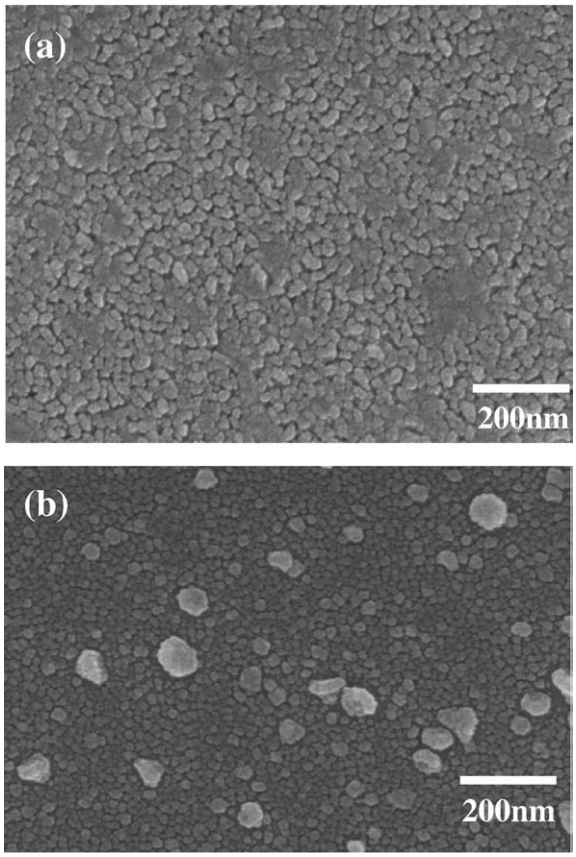

Fig. 2. SEM surface images of undoped ZnO films grown (a) with and (b) without a buffer layer.

Fig. 3 shows the XRD patterns of ZnO undoped thin film and ZnO:Ga films deposited with various TEG flow rates ranging from 1.5 to 10 sccm. As can be seen from Fig. 3, all the films show polycrystalline structure with various crystallographic planes being detected [31]. XRD patterns show that the undoped film and the films deposited with the TEG flow rate lower than 7.5 sccm exhibit grain structures with a dominant orientation of (101). The intensity of (101) peak retains while that of other peaks decrease with increasing TEG flow rate. The crystal plane with a preferential orientation of (101) is most emphasized when the ZnO film was deposited with a TEG flow rate of 7.5 sccm. Then, the dominant growth orientation changes to (100) with a further increase of TEG flow rate to 10 sccm. The results described above demonstrate that Ga-doping plays an important role in resolving the crystal orientations of ZnO films fabricated on glass substrate. It might imply that the amount of Ga elements involved in ZnO film would influence the formation of microstructures therein. In addition, it should be noted that the preferential grain orientation of our films is (101) but not the one of (002) indicated by most other articles. This is considered to be associated with the low-temperature (170 °C) grown buffer, which might have made the (101) plane emerge easily and a detailed study about this is in process.

SEM surface morphology of ZnO:Ga thin films fabricated with various TEG flow rates are shown in Fig. 4. In the same figure, the image taken from undoped film is also presented for comparison. Also, the corresponding cross-sectional images of films are shown in the respective inset of these figures. As the TEG flow rate is increased, several kinds of crystalline grain are observable. Obviously from Fig. 4(a) that undoped ZnO film exhibits a surface morphology full of irregular sheet islands which can be roughly categorized into the larger and the smaller ones according to their sizes. Besides, the surface of undoped film is very rugged as can be seen from the inset in Fig. 4(a). On the other hand, for the ZnO:Ga films fabricated with the TEG flow rates ranging from 1.5 to 5 sccm the sheet shaped grains change into more like 3-dimensionally structured grains with their size distribution becomes more homogeneous. Fig. 4(b), (c) and their insets display respectively the plan-view and cross-sectional images of the 3-dimensionally grained structures described above. Moreover, with a further increase of TEG flow rate to 7.5 sccm, a planar grained structure appears as viewed from Fig. 4(d) and the surface of ZnO:Ga film is relatively smooth as compared the inset of Fig. 4(d) with those of the other figures in Fig. 4. This is considered to be in good agreement with the results presented in Fig. 3 where a predominant growth direction of ZnO:Ga film was resolved when the film was fabricated at a TEG flow rate = 7.5 sccm. Finally, when the ZnO:Ga film growth is conducted with a TEG flow rate of 10 sccm, a pyramid-like structure is observed on top surface as displayed in Fig. 4(e) and further confirmed by the corresponding inset. This is also in accordance with the result presented in Fig. 1 that as the TEG flow rate is increased to 10 sccm, the predominant growth direction of ZnO:Ga film changes from (101) to (100) and the grain structure becomes more complicated than the case with the TEG flow rate = 7.5 sccm, which therefore results in a rough surface again. According to results described above, one can understand that the amount of Ga doped influences the formation of microstructures in the ZnO:Ga films, which agrees well with the XRD measurements. It has also been indicated that excess Ga atoms will react with oxygen atoms to form Ga_2O_3, which is considered to cause the crystalline degradation of ZnO:Ga films [32].

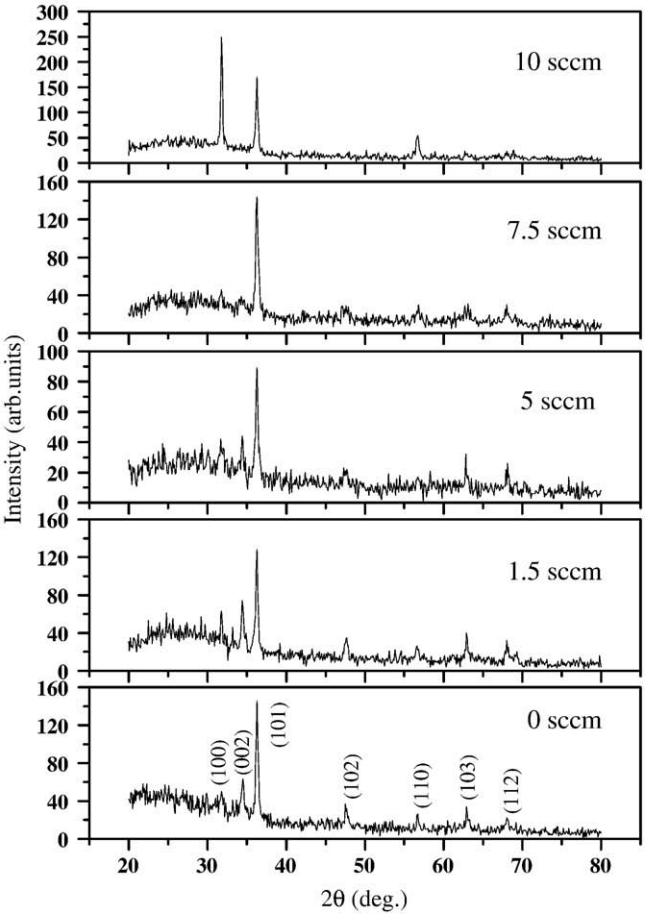

Fig. 3. XRD patterns of undoped ZnO film and ZnO:Ga films fabricated at different TEG flow rates.

Fig. 5 shows the resistivity (r), electron concentration (n) and Hall mobility (μ_H) of undoped ZnO and ZnO:Ga thin films as a function of the TEG flow rate. Gallium is an n-type dopant that replaces zinc atoms or forms interstitial atom, which increases the free-electron concentration in the films. It can be seen that the resistivity of ZnO:Ga thin films are much lower than that can be achieved in normally undoped ZnO. The resistivity of doped films decreases initially with increasing TEG flow rate and achieves a minimum value of 3.6×10^{-4} Ω cm at 7.5 sccm. Then it increases conversely with a further increase of TEG flow rate. Whereas, the electron concentration increases from 6.33×10^{18} to 6.96×10^{20} cm^{-3} with increasing TEG flow rate from 0 to 7.5 sccm and approaches a saturated value after the TEG flow rate is increased to over 7.5 sccm. These results demonstrate that Ga elements can be incorporated in ZnO lattice and an appropriate amount of Ga doped contributes to the doping effect on ZnO films. Otherwise, the Hall mobility increases gradually with increasing TEG flow rate and begins to decrease after reaching a maximum value of 30.4 $cm^2\,V^{-1}\,s^{-1}$ at 7.5 sccm. As is known, the resistivity is affected by both the electron concentration and the Hall mobility but is usually dominated by the electron concentration since there are quite different orders of change for both parameters once the doping amount is varied. The decrease in resistivity with increasing TEG flow rate is therefore due to the doping effect of Ga atoms. While, the increase of resistivity with increasing TEG flow rate to over 7.5 sccm manifests that here the resistivity is not determined by electron concentration but by Hall mobility instead as can be understood by comparing the resistivity, the Hall mobility, and the electron concentration simultaneously in the corresponding regions in Fig. 5. As is reported, the Hall mobility (μ_H) can be expressed as [33]

$$\frac{1}{\mu_H} = \frac{1}{\mu_i} + \frac{1}{\mu_g},$$

where μ_i and μ_g are the mobilities dominated by impurity scattering and grain boundary scattering, respectively. μ_i should decrease with increasing TEG flow rate since the amount of Ga atoms incorporated in ZnO film is increased. Hence, it is reasonable to consider that the

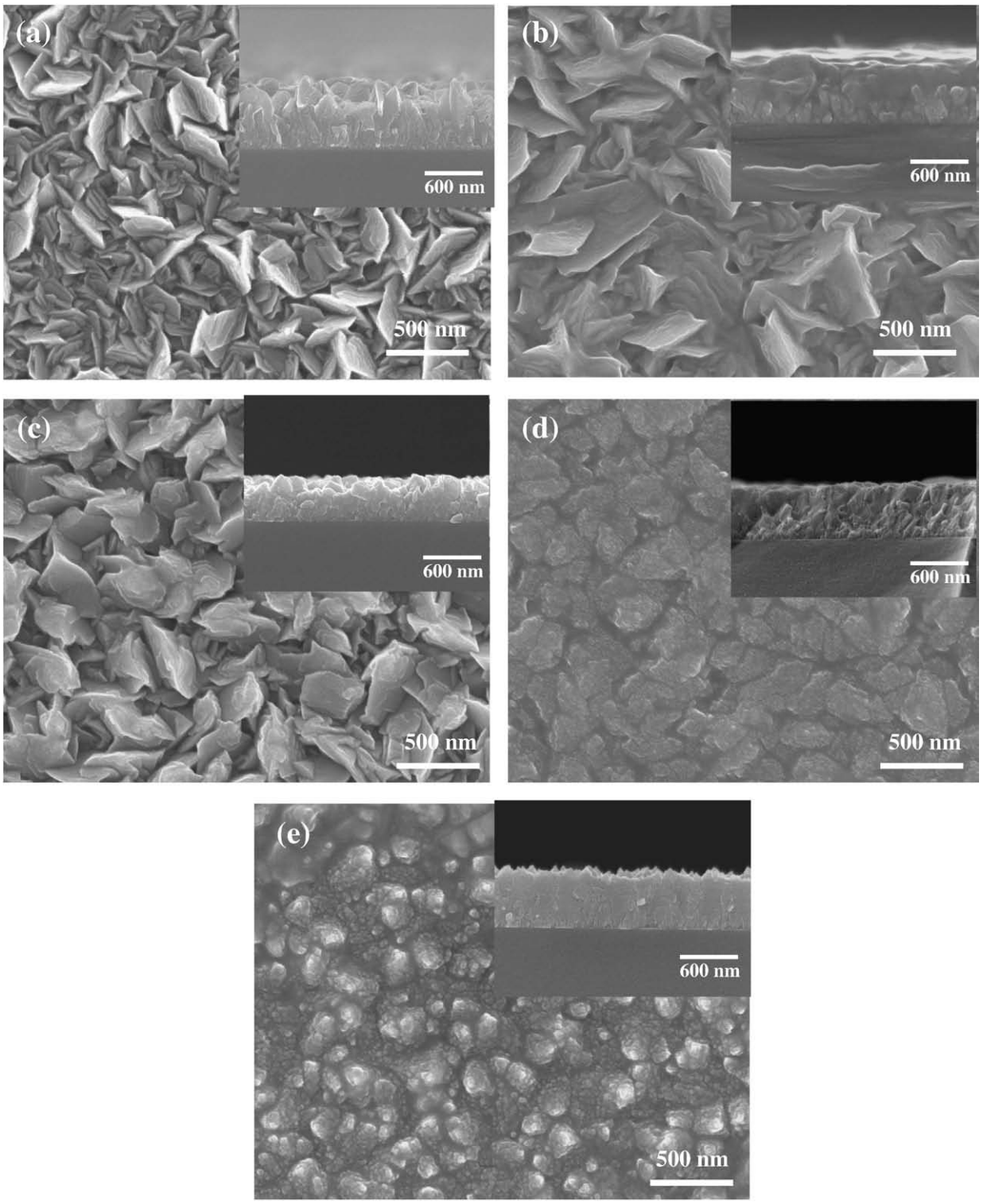

Fig. 4. SEM images of (a) undoped ZnO film and ZnO:Ga films deposited with different TEG flow rates: (b) 1.5, (c) 5, (d) 7.5, and (e) 10 sccm. The inset of each figure shows the corresponding cross-sectional SEM image.

increase of Hall mobility with increasing TEG flow rate is mainly dominated by μ_g. Namely, the increase of Hall mobility with increasing TEG flow rate to 7.5 sccm indicates the dominance of grain boundary scattering. As demonstrated in both XRD and SEM results described above, the grain structure is simplified and exhibits a relatively flat surface as the TEG flow rate is increased to 7.5 sccm. This should be connected to a reduction in the area of grain boundaries, which should have been beneficial for elevating μ_g and therefore μ_H. That is to say, the increase of Hall mobility is due to the decrease of scattering from the grain boundaries. However, a further raise of TEG flow rate to 10 sccm might cause a complex grain structure to appear again and resultantly increase the area of grain boundaries. Therefore, in this case not only the impurity scattering but also the grain boundary scattering would work consistently to make μ_H decrease.

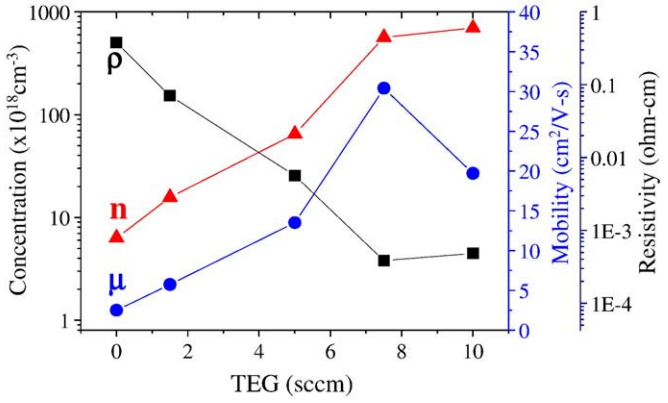

Fig. 5. Resistivity, electron concentration, and mobility of ZnO:Ga films as a function of TEG flow rate.

Fig. 6 shows the transmission spectra in the wavelength range of 300–850 nm for the samples deposited using various TEG flow rates. As the TEG flow rate increases from 0 to 10 sccm, the average transmittance increases from 75% to more than 85% and the absorption edge shifts to a shorter wavelength. The interference fringes in the transmittance curves reveal that the magnitude of the refractive index increases and it is quite evident that the effect of increasing TEG flow rate to above 7.5 sccm is to reduce drastically the film porosity, which is in agreement with the SEM images.

The optical absorption coefficient α as a function of incident photon energy $h\nu$ can be expressed by:

$$(\alpha h\nu)^2 = A\left(h\nu - E_g\right), \tag{1}$$

where A is a constant for a direct interband transition and E_g is the optical bandgap energy. Fig. 7 shows the plots of $(\alpha h\nu)^2$ as a function of $h\nu$ for ZnO:Ga thin films fabricated with various TEG flow rates. The E_g can be estimated by extrapolating the linear portion of the curve to intercept the energy axis (with $\alpha = 0$) and is found to vary from 3.26 to 3.71 eV as the TEG flow rate is increased from 0 to 10 sccm, as demonstrated in the inset of Fig. 5. A blue shift of the absorption edge due to an increase of E_g is observable when the TEG flow rate is increased, which is known as the effect of Burstein–Moss shift [34,35]. These results indicate that by modulating the TEG flow rate to higher than 7.5 sccm for Ga-doping n-type degenerate ZnO films with their

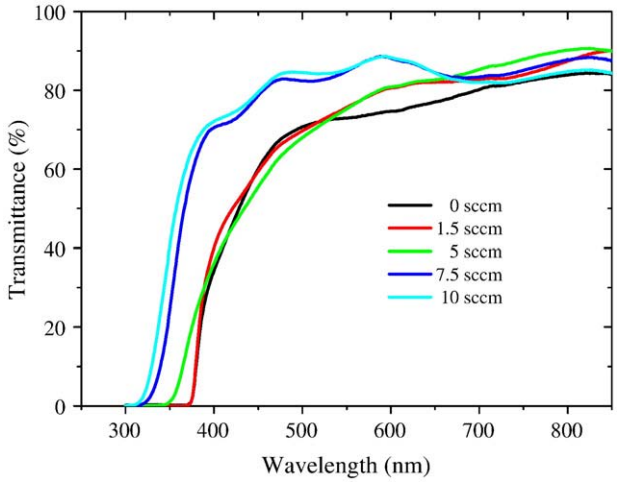

Fig. 6. Transmittance of undoped ZnO film and ZnO:Ga films fabricated with various TEG flow rates.

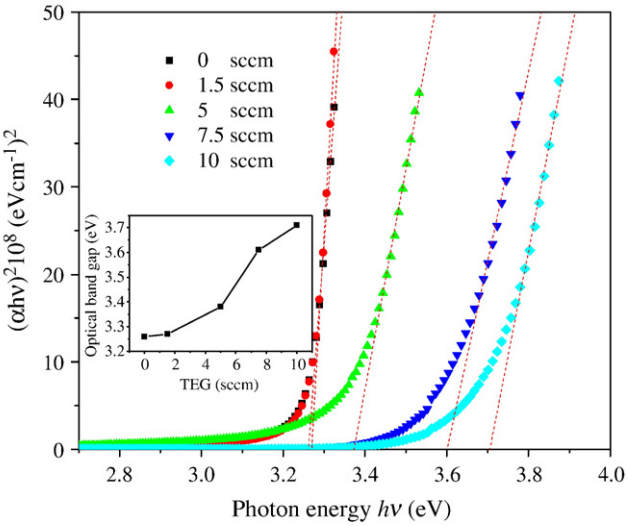

Fig. 7. The absorption edge of the ZnO:Ga films fabricated with various TEG flow rates. The inset shows the variation of optical band gap as a function of TEG flow rate.

electron density over 5.0×10^{20} cm^{-3} can be prepared. In such films, the optical bandgap energy has been increased by about 10.7–13.8%.

4. Conclusions

ZnO:Ga films have been grown on glass substrates by AP-MOCVD technique using TEG as the doping gas. It is found that Ga elements can be effectively employed to act as donors, which can be activated to afford electron concentrations higher than 5.0×10^{20} cm^{-3} at TEG flow rates of over 7.5 sccm. In addition, Ga-doping influences the formation of microstructures in ZnO. The preferential orientation of grain structures of ZnO:Ga films is (101) when the films are fabricated at TEG flow rates ≤7.5 sccm; however, it changes to (100) when the film is deposited at a TEG flow rate >7.5 sccm. A smooth surface morphology is achieved for the film deposited at the TEG flow rate = 7.5 sccm. In particular, it is found that the mobility is dominated by the grain boundary scattering when the TEG flow rate is lower than 7.5 sccm, while it is dominated by both the ionized impurity and the grain boundary scattering when the TEG flow rate is higher than 7.5 sccm. This phenomenon has made a highest mobility of 30.4 cm^2 V^{-1} s^{-1} be obtained at the TEG flow rate of 7.5 sccm. Moreover, both the variations of electron concentration and mobility resolve a minimum resistivity of 3.6×10^{-4} Ω cm obtained at TEG flow rate = 7.5 sccm. On the other hand, the Ga-doping technique has been shown to produce degenerate n-type ZnO films possible, which causes the average transmittance of both ZnO films deposited at TEG flow rates of 7.5 and 10 sccm to reach 85%. Besides, as the TEG flow rate is increased from 0 to 10 sccm, the absorption edge shifts to shorter wavelength and the optical band gap increases from 3.26 to 3.71 eV. Conclusively, the Ga-doping can be used to produce low-resistivity and high-transparency n-type ZnO films. These films can be used as a window layer for thin-film solar cells or the transparent electrodes for OLEDs (organic light-emitting diodes) as a replacement for ITO electrode and contribute to an improvement in the performance of these devices.

Acknowledgements

The authors would like to thank the National Science Council of the Republic of China, Taiwan, for financially supporting this research under Contract No. NSC 97-2623-7-033-002-NU. The Institute of Nuclear Energy Research (INER) is appreciated for its extensive technical assistance.

References

[1] B. Rech, H. Wagner, Appl. Phys. A 69 (1999) 155.
[2] A. Shimizu, S. Chaisitsak, T. Sugiyama, A. Yamada, M. Konagai, Thin Solid Films 361/362 (2000) 193.
[3] J.C. Lee, K.H. Kang, S.K. Kim, K.H. Yoon, I.J. Park, J. Song, Sol. Energy Mater. Sol. Cells 64 (2000) 185.
[4] A.F. Kohan, G. Ceder, D. Morgan, C.G. Van de Walle, Phys. Rev. B 61 (2000) 15019.
[5] K.-K. Kim, S. Niki, J.-Y. Oh, J.-O. Song, T.-Y. Seong, S.-T. Park, S. Fujita, S.-W. Kim, J. Appl. Phys. 97 (2005) 066103.
[6] T. Makino, Y. Segawa, S. Yoshida, A. Tsukazaki, A. Ohtomo, M. Kawasaki, Appl. Phys. Lett. 85 (2004) 759.
[7] T. Minami, H. Nanto, S. Takata, Jpn. J. Appl. Phys. 23 (1984) L280.
[8] K.L. Chopra, S. Major, D.K. Pandya, Thin Solid Films 102 (1983) 1.
[9] Y. Li, G.S. Tompa, S. Liang, C. Gorla, Y. Lu, John Doyle, J. Vac. Sci. Technol. A 15 (1997) 1063.
[10] X.L. Chen, B.H. Xu, J.M. Xue, Y. Zhao, C.C. Wei, J. Sun, Y. Wang, X.D. Zhang, X.H. Geng, Thin Solid Films 515 (2007) 3753.
[11] K.Y. Cheong, Norani Muti, S. Roy Ramanan, Thin Solid Films 410 (2002) 142.
[12] K.T.R. Reddy, T.B.S. Reddy, I. Forbes, R.W. Miles, Surf. Coat. Technol. 151/152 (2002) 110.
[13] H. Gomeza, A. Maldonadoa, M. de la L. Olveraa, D.R. Acosta, Sol. Energy Mater. Sol. Cells 87 (2005) 107.
[14] V. Assuncao, E. Fortunato, A. Marquesa, H. Á guasa, I. Ferreiraa, M.E.V. Costab, R. Martinsa, Thin Solid Films 427 (2003) 401.
[15] X. Yu, J. Ma, F. Ji, Y. Wang, X. Zhang, C. Cheng, H. Ma, J. Cryst. Growth 274 (2005) 474.
[16] X. Yu, J. MaT, F. Ji, Y. Wang, X. Zhang, H. Ma, Thin Solid Films 483 (2005) 296.
[17] Q.B. Ma, Z.Z. Ye, H.P. He, S.H. Hu, J.R. Wang, L.P. Zhu, Y.Z. Zhang, B.H. Zhao, J. Cryst. Growth 304 (2007) 64.
[18] Z.F. Liu, F.K. Shan, Y.X. Li, B.C. Shin, Y.S. Yu, J. Cryst. Growth 259 (2003) 130.
[19] S.J. Henley, M.N.R. Ashfold, D. Cherns, Surf. Coat. Technol. 177/178 (2004) 271.
[20] H. Kato, M. Sano, K. Miyamoto, T. Yao, J. Cryst. Growth 237/239 (2002) 538.
[21] T. Yamamoto, T. Sakemi, K. Awai, S. Shirakata, Thin Solid Films 451/452 (2004) 439.
[22] J. Hu, R.G. Gordon, J. Appl. Phys. 72 (1992) 5381.
[23] V. Khranovskyy, U. Grossner, V. Lazorenko, G. Lashkarev, B.G. Svensson, R. Yakimova, Superlattices Microstruct. 39 (2006) 275.
[24] J.D. Ye, S.L. Gu, S.M. Zhu, S.M. Liu, Y.D. Zheng, R. Zhang, Y. Shi, H.Q. Yu, Y.D. Ye, J. Cryst. Growth 283 (2005) 279.
[25] E.W. Forsythe, Yongli GaO, L.G. Provost, G.S. Tompa, J. Vac. Sci. Technol. A 17 (1999) 4.
[26] H. Sato, T. Minami, S. Takata, M. Ishii, Thin Solid Films 246 (1994) 65.
[27] Y. Lia, G.S. Tompa, S. Liang, C. Gorla, Y. Lu, J. Doyle, J. Vac. Sci. Technol. A 15 (1997) 1063.
[28] B. Hahn, G. Heindel, E. Pschorr-Schoberer, W. Gebhardt, Semicond. Sci. Technol. 13 (1998) 788.
[29] J.D. Ye, S.L. Gu, S.M. Zhu, S.M. Liu, Y.D. Zheng, R. Zhang, Y. Shi, H.Q. Yu, Y.D. Ye, J. Cryst. Growth 283 (2005) 279.
[30] N. Nishimoto, T. Yamamae, T. Kaku, Y. Matsuo, K. Senthilkumar, O. Senthilkumar, J. Okamoto, Y. Yamada, S. Kubo, Y. Fujita, J. Cryst. Growth 310 (2008) 5003.
[31] J.I. Langford, A. Boultif, J.P. Auffredic, D. Louer, J. Appl. Crystallogr. 26 (1993) 22.
[32] N. Roberts, R.P. Wang, A.W. Sleight, W.W. Warren Jr., Phys. Rev. B 57 (1998) 5734.
[33] S. Ghosh, A. Sarkar, S. Chaudhuri, A.K. Pal, Thin Solid Films 205 (1991) 64.
[34] E. Burstein, Phys. Rev. 93 (1954) 632.
[35] T.S. Moss, Proc. Phys. Soc. London Ser. B 67 (1954) 775.